SPECIAL TOPIC — International Conference on Nanoscience & Technology, China 2013

Adsorptions and diffusions of carbon atoms on the surface and in the subsurface of Co (200): A first-principles density-functional study*

Qiao Liang(乔 靓)[a)b)c)], Wang Shu-Min(王淑敏)[a)d)], Zhang Xiao-Ming(张晓明)[a)], Hu Xiao-Ying(胡小颖)[b)], Zeng Yi(曾 毅)[a)†], and Zheng Wei-Tao(郑伟涛)[a)‡]

[a)] *College of Materials Science and Engineering, Jilin University, Changchun* 130012, *China*
[b)] *College of Science, Changchun University, Changchun* 130022, *China*
[c)] *State Key Laboratory of Theoretical and Computational Chemistry, Jilin University, Changchun* 130012, *China*
[d)] *Light Industry College, Liaoning University, Shenyang* 110036, *China*

(Received 4 September 2013; revised manuscript received 13 February 2014; published online 10 June 2014)

First-principles calculations based on density functional theory are used to investigate the adsorptions and diffusions of carbon atoms on the surface and in the subsurface of Co (200). The preferred site for the carbon atom on the surface is the hollow site, and the preferred site in the subsurface is the octahedral site. There is charge transfer from the surface to the adsorbed carbon atom, and for the most favorable adsorbed structure the charge transfer is largest. Moreover, the energy barriers for the diffusions of carbon atoms on the surface and from the surface into the subsurface and then back to the surface are calculated in detail. The results indicate that the energy barrier for the diffusion of carbon atoms on the surface is comparable to that from the subsurface to the surface. The results imply that both the direct surface nucleation and the surface segregation from Co bulk can be observed in the chemical vapor deposition growth of graphene on Co (200) substrate, which can gain a new insight into the growth mechanism of graphene.

Keywords: adsorption, diffusion, carbon, Co surface, first-principles calculations

PACS: 68.43.Fg, 68.43.Jk, 71.15.Mb **DOI:** 10.1088/1674-1056/23/8/086802

1. Introduction

Graphene possesses remarkable fascinating properties that stimulate a vast amount of research in the fields of materials science,[1,2] since it was isolated in 2004.[3] Nowadays, mechanical exfoliation,[3] epitaxial growth on SiC,[4] reduction of chemically exfoliation graphene oxide,[5] and chemical vapor deposition (CVD)[6] have been used to produce graphene. Among these methods, CVD is superior to other methods due to the possibility to produce a large size of graphene. Various metals, such as Ni and Cu, have been used for the synthesis of graphene.[7,8] However, using these metal substrates, a relatively high temperature or a long time is strictly required. Recently, Co film is used to synthesize large-area and high-mobility graphene.[9,10] In our group, graphene with good optical transmittance has been synthesized on polycrystalline Co film at a relatively low temperature for a shorter reaction time.[11]

First-principles density-functional theory (DFT) has been widely used in the understanding of the CVD growth of carbon nanomaterials on metal substrates. First, the dehydrogenation of the gas precursor over the metal substrate is performed to form carbon species (CH_x). The dehydrogenation energetics of carbon-containing gas on a metal substrate is studied, such as CH_4 on Cu substrate.[12] Then, the carbon species can diffuse on the metal surface or into the metal substrate. During the annealing, the carbon atoms can be segregated onto the surface. Finally, the carbon clusters can be formed on the metal substrate and then transform into the sp^2 carbon network. It has been found that the carbon clusters can be formed on Ni (111) and Ir (111) and then coalesce on the terrace and near the step edge.[13,14] Moreover, generally the diffusion of carbon atoms in the initial stage is regarded as a crucial step for the overall growth of carbon nanomaterials.[15,16]

Theoretical calculations can provide detailed information about the interaction between the carbon atom and the metal surface.[16–18] The adsorptions of carbon atoms on Ni, Cu, and Co surfaces have been theoretically studied,[16,18–23] and the energy barriers for the diffusion of carbon atoms on Ni and Co (111) surfaces have been identified.[16,18,19] Moreover, the diffusion of carbon atoms from the surface to the subsurfaces of Ni, Fe, and Co have also been studied to evaluate the growth of carbon nanomaterials.[16,19,20,24–26]

As for the synthesis of graphene on Co substrate, the face-centered cubic (fcc) and hexagonal close-packed (hcp)

*Project supported by the National Natural Science Foundation of China (Grant Nos. 51002014, 51202017, and 51372095), the Research Fund for the Doctoral Program of Higher Education of China (Grant No. 20120061120039), the Funds from the Science and Technology Department of Jilin Province, China (Grant Nos. 20120745 and 20130101029JC), the Funds from the Department of Education of Jilin Province, China (Grant No. 2013279), and the Youth Science Research Foundation of Liaoning University, China (Grant No. 2013LDQN20).

†Corresponding author. E-mail: zengyi@jlu.edu.cn
‡Corresponding author. E-mail: wtzheng@jlu.edu.cn

© 2014 Chinese Physical Society and IOP Publishing Ltd

Co films are commonly used.[9–11] In order to understand our recent synthesis of graphene using fcc Co film,[11] we only consider the fcc Co in the following study. As is well known, Co (111) and (200) surfaces can exist stably. However, although there exist several studies about the adsorption and diffusion of carbon atoms on the surface or in the subsurface of Co (111),[18,19,23] to the best of our knowledge, there are no reports on the Co (200) surface, especially the diffusion of carbon atoms into the subsurface. Therefore, it is of great significance to study the interaction between the carbon atom and the Co (200) surface, which can provide the growth mechanism of graphene on Co film from the theoretical point of view.

In the present work, the adsorptions and diffusions of carbon atoms on the surface and in the subsurfaces of Co (200) are investigated using first-principles DFT calculations. The lowest energy positions for the carbon atom on the surface and in the subsurface are determined. Moreover, a comparative study of the carbon atom on the surface to diffuse, to penetrate from the surface into the subsurface and then to spill over back to the surface is performed in detail, and the energy barriers for the diffusion are obtained to reveal the initial step of growth of graphene on Co (200) surface.

2. Calculation methods

The spin-polarized calculations are performed using the first-principles DFT code CASTEP.[27,28] The exchange correlation functional is treated within the generalized gradient approximation and parameterized by Perdew–Burk–Ernzerhof formula.[29] The Brillouin-zone integrations are approximated using the special k-point sampling of Monhkorst–Pack scheme.[30] The cutoff energy is set to be 400 eV.

The Co (200) surface is modeled as a slab, which contains a 2×2 surface with six Co layers and is separated from its periodic images by a vacuum layer of 15 Å. The top view of the surface is shown in Fig. 1(a). The surface is represented by three upper Co layers, and the three lower Co layers are fixed to simulate the bulk layers.

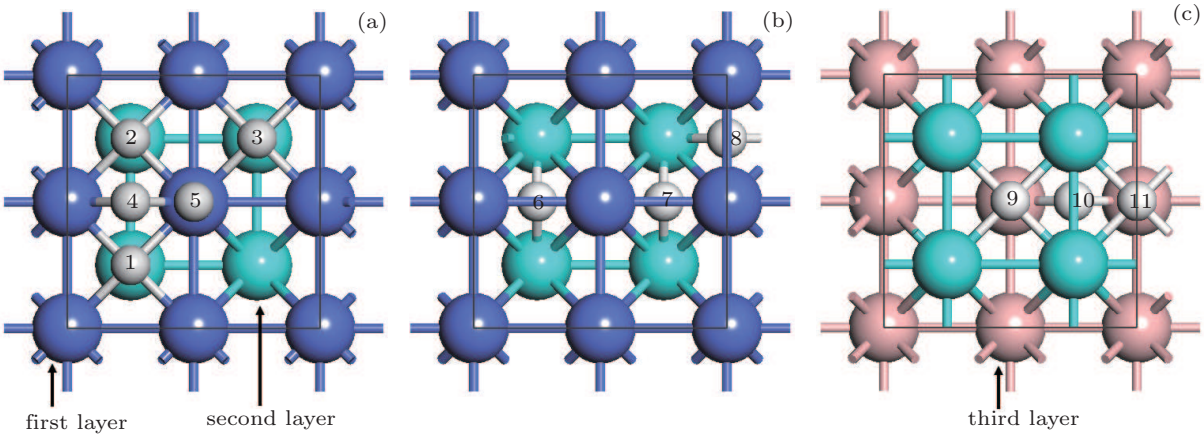


Fig. 1. (color online) Schematic illustrations of the adsorption sites for carbon atom (a) on the surface, (b) in the first subsurface, and (c) in the second subsurface of Co (200). The Co atoms in the first, second, and third layers are represented as large spheres, and the carbon atom is represented as small white sphere. For the sake of clarity, the first Co layer is not shown in panel (c). The adsorption sites 1 to 5 in panel (a) denote the H-1, H-2, H-3, bridge, and top sites, respectively. The adsorption sites 6 to 8 in panel (b) denote the T(I)-1, T(I)-2, and T(I)-3 sites, respectively. The adsorption sites 9 to 11 in panel (c) denote the O(II)-1, T(II), and O(II)-2 sites, respectively.

The carbon atom is originally placed at three high-symmetry positions of the Co (200) surface with a coverage of 25%: the hollow (H), bridge, and top sites as shown in Fig. 1(a). For Co bulk, there exist two kinds of interstitial sites: the octahedral (O) and tetrahedral (T) sites. In the first subsurface of Co (200), four Co atoms in the first layer and one Co atom in the second layer form a Co_5 half octahedral (HO) cavity, and for the adsorption of carbon atoms in the first subsurface, the HO and T(I) sites are considered. For the adsorption in the second subsurfaces, the O(II) and T(II) sites are considered. The above adsorption sites in the subsurface are illustrated in Figs. 1(b) and 1(c). Furthermore, the energy barriers for the carbon atom on the Co (200) surface to diffuse, to penetrate into the subsurfaces, and then to spill over back to the surface are identified using the linear synchronous transit/quadratic synchronous transit (LST/QST) method.[31]

3. Results and discussion

3.1. Adsorption of carbon atom

The adsorbed Co (200) surfaces are fully relaxed, and the calculated adsorption energies and the corresponding structural parameters are listed in Table 1. The adsorption energy E_A for the carbon atom to adsorb on the Co (200) surface is defined as follows:

$$E_A = E(\mathrm{Co+C}) - E(\mathrm{Co}) - E(\mathrm{C}), \quad (1)$$

where E(Co+C), E(Co), and E(C) are the total energies of the adsorbed surface, the clean surface, and an isolated carbon atom, respectively. It can be seen that the adsorption energies are all negative, which indicates that the adsorption process is exothermic and the carbon atom can adsorb on the Co (200) surface stably. The calculated adsorption energies are in a range from −4.84 eV to −7.82 eV, indicating that the adsorption is a strong chemical adsorption. The adsorption energy of −7.82 eV at H site is lower than those on other sites, which shows that the preferred adsorption site is the H site. The preference of carbon atoms at the H site of the Co (200) surface is similar to the adsorptions on Ni and Cu (100) surfaces.[21]

Table 1. Calculated values of parameters of carbon atom adsorbed on Co (200) surface: adsorption energy E_A, the average Co–Co bond length d_{Co-Co} of the first Co layer near the adsorption site, the average Co–C bond length d_{Co-C}, the perpendicular distance h between the adsorbed carbon atom and the nearest Co atom, and the charge transfer Δq.

	E_A/eV	d_{Co-Co}/Å	d_{Co-C}/Å	h/Å	Δq[a)]/e
H	–7.82	2.64	1.89	0.32	0.74
Bridge	–5.86	2.56	1.75	1.19	0.42
Top	–4.84	2.51	1.63	1.63	0.24

[a)] With respect to the charge transfer from the surface to the adsorbed carbon atom.

At the preferred H site, the coordination number is the largest and the carbon atom has the largest number of neighboring Co atoms to bond width. Compared with the bond length 2.51 Å of the Co–Co bond in Co bulk, the lattice of the surface can expand due to the adsorption of carbon atoms: the distortion for the adsorption at the H site is largest. At the H site, the adsorbed carbon atom bonds to the four nearest surface Co atoms, each with a bond length of 1.89 Å. This bond length is longer than those at other adsorption sites due to the larger coordination number of the carbon atom at the H site. Furthermore, the perpendicular distance of the carbon atom to the Co (200) surface is shortest at the H site, and the adsorbed carbon atom can also bond to the Co atom in the second layer right below the adsorption site with a Co–C bond length of 2.06 Å.

It is known that Co has a higher carbon solubility, and the dissolved carbon atoms will occupy the interstitial O and T sites. For the first subsurface of Co (200), the carbon atoms are initially placed at the HO and T(I) sites. For the second subsurface, the O(II) and T(II) sites are considered. It is found that the carbon atom initially placed in the HO site moves out of the HO site to the surface H site after the geometrical optimization. Therefore, the carbon atom can only be dissolved at the T(I) site of the first subsurface and the O(II) and T(II) sites of the second subsurface.

The adsorption energy for the dissolution of a carbon atom in the subsurface of Co (200) can also be calculated using formula (1), and the calculated values are listed in Table 2. It can also be seen that the dissolution of a carbon atom in the Co subsurface is an exothermic process. The calculated adsorption energy for the O(II) site is significantly lower than those for T(I) and T(II) sites, which indicates that the adsorption in the O(II) site is the most stable and those in the T sites are metastable. This can be ascribed to (i) the higher coordination number of the carbon atom at the O(II) site and (ii) the relatively large volume of the O(II) site. The dissolution of a carbon atom in the subsurface can expand the volume of the interstitial sites, which can be seen from the enlarged Co–Co bond lengths as listed in Table 2. After the incorporation of the carbon atom, the O(II) site remains octahedral, while the T sites distort remarkably due to their smaller volumes. When the carbon atom is adsorbed at the O(II) site, the length of the Co–C bond is similar to that when the carbon atom is adsorbed on the surface H site. A comparison of the adsorption energies for the carbon atom adsorbed at different locations on the surface listed in Table 1 shows that the carbon atom prefers the surface H site to the interstitial sites in the subsurface. Although Co has a high carbon solubility, the preference of the carbon atom on the surface can be ascribed to the fact that the dissolution of the carbon atom in the subsurface will lead to a large structural distortion and induce the strains in the structure as mentioned above. The adsorptions of carbon atoms on Ni (100) and Fe (100) surfaces also show the same trends.[20,24] The preference of the adsorption on the surface can explain where the carbon atom will go after the dissociation of the precursor from the viewpoint of the atomic scale, and this can be used to reveal the growth mechanism of graphene on Co substrate later.

Table 2. Calculated values of parameters for the adsorption of a carbon atom in the subsurface of Co (200): adsorption energy E_A, the average Co–Co bond length d_{Co-Co} near the adsorption site, the average Co–C bond length d_{Co-C}, and the charge transfer Δq.

	E_A/eV	d_{Co-Co}/Å	d_{Co-C}/Å	Δq[a)]/e
T(I)	–4.89	2.77,[b)] 2.62,[c)] 3.04[e)]	1.80	0.61
O(II)	–6.61	2.64,[c)e)] 2.67[f)]	1.87	0.72
T(II)	–4.74	2.70,[c)] 2.69,[d)] 3.00[f)]	1.78	0.58

[a)] With respect to the charge transfer from the surface to the adsorbed carbon atom.

[b)c)d)] With respect to the Co–Co bonds in the first, second, and third Co layers, respectively.

[e)f)] With respect to the Co–Co bonds between the first and second, and the second and third Co layers, respectively.

The values of Mulliken charge transfer Δq from the Co (200) surface to the adsorbed carbon atom are listed in Tables 1 and 2. It can be seen that the adsorbed carbon atom behaves like an electronegative species causing a net charge to transfer from the Co atoms to the carbon atom and resulting in the charge redistribution of the Co surface. The charge transfers for the adsorption of the carbon atom on the surface H site and at the O(II) site of the subsurface are largest, respectively. A correlation between the charge transfer and the adsorption

energy can be observed that the lower the adsorption energy, the larger the charge transfer is.

3.2. Diffusion of carbon atom

The diffusions of carbon atoms on Co (200) surface and from the surface to the subsurface are initial steps in the CVD growth of graphene. As shown above, the H site is the most favorable site, and the bridge and top sites are metastable sites. By taking into account the symmetry, the diffusion of a carbon atom is simply a hopping between these sites. The schematic representations of the diffusion 1 of carbon atoms on the surface are illustrated in Fig. 2 through four different pathways. It is found that the diffusion 1 of carbon atoms from the top site directly to the H-1 site is automatically without any energy barrier. The situation is the same as that for diffusion 2 if the carbon atom diffuses from the top site first to the bridge site and then to the H-1 site. Moreover, there are two diffusion paths between two neighboring H sites, and the energy barriers for the diffusions are shown in Fig. 2. For diffusions 3 and 4 across the bridge and top sites, the energy barriers are 1.99 eV and 3.08 eV, respectively. The energy barriers of the diffusion of carbon atoms on the Co (200) surface are lower than those on the Ni (100) surface.[20] It can be seen that the diffusion across the bridge site has the lowest energy barrier, and hence the carbon atom has the highest mobility. Therefore, the diffusion of carbon atoms on the surface can happen by hopping between H sites through the bridge site.

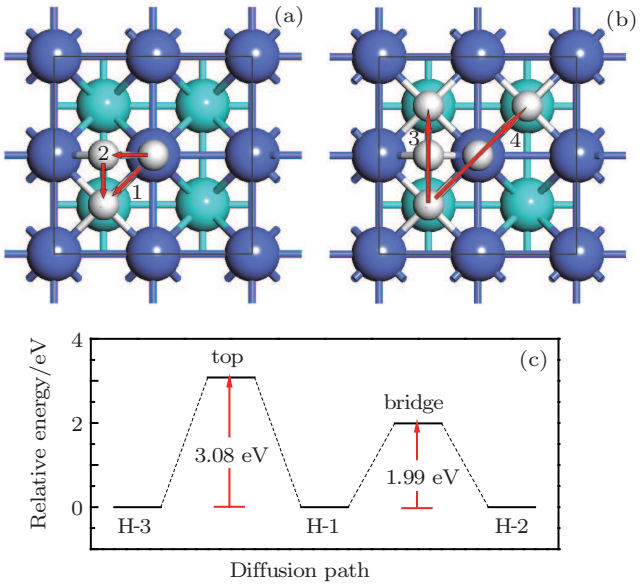


Fig. 2. (color online) (a) and (b) Schematic representations of the diffusions of carbon atoms on the surface along four different pathways. (c) Relative energy versus diffusion path between H sites through the bridge and top sites.

To reveal the initial growth of graphene on the Co (200) surface, the diffusions of carbon atoms from the surface into the first and second subsurfaces are investigated to compare with the diffusion on the surface. Based on the identified preferential adsorption sites for carbon atoms, three possible diffusion paths are evaluated for the carbon atom to penetrate from the surface into the subsurface and then go back to the surface. The schematic representations of the diffusion pathways and the corresponding energy barriers are shown in Figs. 3–5. In pathway 5, the carbon atom at surface H-1 site diffuses to the next surface H-2 site through an adjacent tetrahedral T(I)-1 site of the first subsurface via a face of the half-octahedron as shown in Fig. 3. The calculated energy barrier for pathway 5 is 2.85 eV, which is larger than the energy barrier of pathway 3 through the surface diffusion. It indicates that for the diffusion of a carbon atom between two neighboring H sites, the surface diffusion is more favorable than diffusion through the first subsurface.

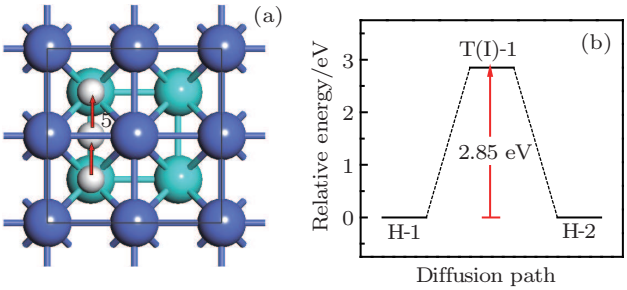


Fig. 3. (color online) (a) Schematic representation and (b) relative energy versus diffusion path of a carbon atom through the tetrahedral site of the first subsurface.

Moreover, for pathway 6, the carbon atom goes from the surface H-1 site into the O(II)-1-site of the second subsurface through the T(I)-1 site and then spills out through the T(I)-2 site to the surface H-3 site. The schematic pathway of the diffusion and the overall energy barriers are shown in Fig. 4. The energy barrier for the carbon atom migration from the H-1 site to O(II)-1 site is 2.85 eV, and the reverse process of the carbon atom back to the surface H-3 site has an energy barrier of 1.70 eV. This indicates that the segregation of the carbon atom from the subsurface to the surface is exothermal, with the energy change being 1.15 eV, and energetically favorable.

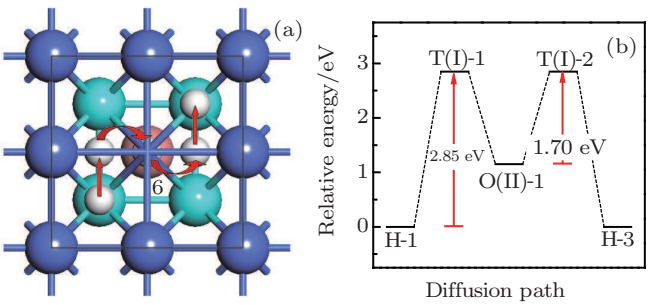


Fig. 4. (color online) (a) Schematic representation and (b) relative energy versus diffusion path of a carbon atom through the octahedral site of the second subsurface. For the sake of clarity, the Co atom in the first layer composed of the octahedral site is not shown.

Furthermore, pathway 7 of the diffusion of the carbon atom in the subsurface is also investigated, and the pathway is

designed for the carbon atom to migrate from the O(II)-1 site to the nearest O(II)-2 site through the T(II) site between them. The overall pathway H-1 $\xrightarrow{\text{T(I)-1}}$ O(II)-2 $\xrightarrow{\text{T(II)}}$ O(II)-2 $\xrightarrow{\text{T(I)-3}}$ H-3 and the calculated energy barriers are shown in Fig. 5. It can be seen that the diffusion of the carbon atom between two O(II) sites in the second subsurface need to overcome an energy barrier of 1.87 eV. It can be seen from the energy barriers of pathways 5 to 7 that the carbon atom diffuses slowly from the surface to the subsurface because of the strong surface effects, while the diffusion in the subsurface is relatively fast due to the lower energy barrier.

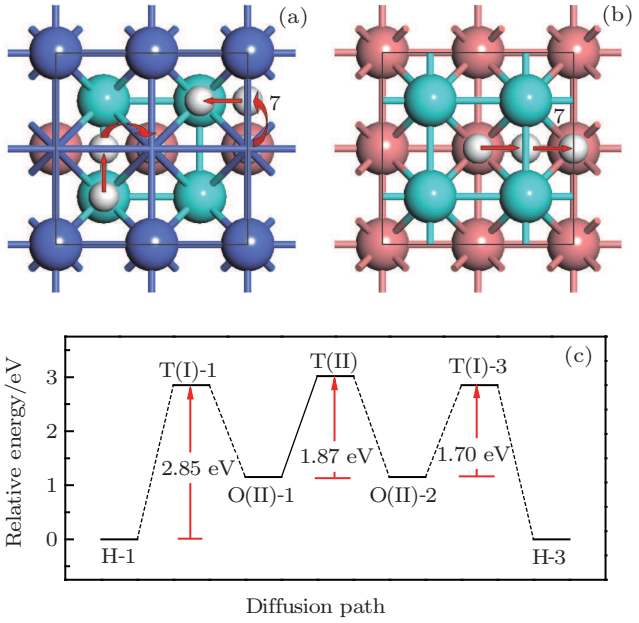


Fig. 5. (color online) (a) and (b) Schematic representations of the diffusion of carbon atoms between octahedral sites in the second subsurface. (c) Relative energy versus diffusion path of the carbon atom. For the sake of clarity, the Co atoms in the first layer composed of the octahedral sites are not shown in panel (a), and the first Co layer is not shown in panel (b) either.

Although the above results do not directly show the growth process of graphene on the Co (200) substrate, they can provide important information concerning the initial step of the growth. It can be seen that the carbon atom prefers adsorbing on the surface H site to adsorbing in the interstitial sites of the subsurface. The topmost layer Co atoms significantly restrain the diffusion of the carbon atom from the surface into the subsurface with a higher energy barrier. In fact, in the exact, high temperature fabrication process, the carbon atoms are dissolved unavoidably in the subsurface of Co bulk. The energy barriers for the carbon atom either in the subsurface or from the subsurface to the surface are slightly lower than that for the diffusion on the surface. Therefore, we think that in the actual experiments of fabrication of graphene on the Co (200) substrate, the direct surface nucleation and two-dimensional growth as well as the surface segregation from the Co bulk can happen simultaneously, which is different from the growth mechanism of graphene on Ni and Cu.

4. Conclusions

In this paper, first-principles DFT calculations are performed to investigate the adsorptions and diffusions of carbon atoms on the surface and in the subsurface of Co (200). For the case of on-the-surface, the preferential adsorption site is the hollow site. While for the case of in-the-subsurface, the preferential adsorption site is the octahedral site. Based on the adsorption energies, the carbon atom prefers staying on the surface to residing in the subsurface. The analysis for the Mulliken charge transfer indicates that there is charge transfer from the surface to the adsorbed carbon atom. Moreover, seven possible diffusion pathways are designed to evaluate the diffusion of the carbon atom. It is found that the diffusion of the carbon atom on the surface is more likely to happen between two neighboring hollow sites across the bridge site with an energy barrier of 1.99 eV. The penetration of the carbon atom from the surface hollow site into the octahedral site of the subsurface is relatively slow due to the higher energy barrier of 2.85 eV. Once the carbon atom is dissolved in the subsurface, the diffusion in the subsurface and the spilling out segregation to the surface are relatively easy to occur, and the energy barrier is comparable to that on the surface. Our results provide important information about the initial step of the growth of graphene on Co (200), where both the direct surface nucleation and the surface segregation from the Co bulk can happen simultaneously in the CVD synthesis, which is conducible to understanding the growth mechanism of graphene.

References

[1] Geim A K and Novoselov K S 2007 *Nat. Mater.* **6** 183
[2] Zhao J, Zhang G Y and Shi D X 2013 *Chin. Phys. B* **22** 057701
[3] Novoselov K S, Geim A K, Morozov S V, Jiang D, Zhang Y, Dubonos S V, Grigorieva I V and Firsov A A 2004 *Science* **306** 666
[4] Wang D C, Zhang Y M, Zhang Y M, Lei T M, Guo H, Wang Y H, Tang X Y and Wang H 2012 *Chin. Phys. B* **21** 038102
[5] Stankovich S, Dikin D A, Piner R D, Kohlhaas K A, Kleinhammes A, Jia Y Y, Wu Y, Nguyen S T and Ruoff R S 2007 *Carbon* **45** 1558
[6] Wang W R, Zhou Y X, Li T, Wang Y L and Xie X M 2012 *Acta Phys. Sin.* **61** 038702 (in Chinese)
[7] Park H J, Meyer J, Roth S and Skakalova V 2010 *Carbon* **48** 1088
[8] Ismach A, Druzgalski C, Penwell S, Schwartzberg A, Zheng M, Javey A, Bokor J and Zhang Y G 2010 *Nano Lett.* **10** 1542
[9] Ago H, Ito Y, Mizuta N, Yoshida K, Hu B S, Orofeo C M, Tsuji M, Ikeda K and Mizuno S 2010 *ACS Nano* **4** 7407
[10] Ramon M E, Gupta A, Corbet C, Ferrer D A, Movva H C P, Carpenter G, Colombo L, Bourianoff G, Doczy M, Akinwande D, Tutuc E and Banerjee S K 2011 *ACS Nano* **5** 7198
[11] Wang S M, Pei Y H, Wang X, Wang H, Meng Q N, Tian H W, Zheng X L, Zheng W T and Liu Y C 2010 *J. Phys. D: Appl. Phys.* **43** 455402
[12] Zhang W H, Wu P, Li Z Y and Yang J L 2011 *J. Phys. Chem. C* **115** 17782
[13] Gao J F, Yip J, Zhao J J, Yakobson B I and Ding F 2011 *J. Am. Chem. Soc.* **133** 5009
[14] Wu P, Jiang H J, Zhang W H, Li Z Y, Hou Z H and Yang J L 2012 *J. Am. Chem. Soc.* **134** 6045
[15] Louchev O A, Laude T, Sato Y and Kanda H 2003 *J. Chem. Phys.* **118** 7622
[16] Zhu Y A, Dai Y C, Chen D and Yuan W K 2007 *Surf. Sci.* **601** 1319

[17] Wei H Y, Xiong X L, Song H T and Luo S Z 2010 *Chin. Phys. Lett.* **27** 097102
[18] Hofmann S, Csanyi G, Ferrari A C, Payne M C and Robertson J 2005 *Phys. Rev. Lett.* **95** 036101
[19] Li B H, Zhang Q J, Chen L, Cui P and Pan X Q 2010 *Phys. Chem. Chem. Phys.* **12** 7848
[20] Zhu Y A, Zhou X G, Chen D and Yuan W K 2007 *J. Phys. Chem. C* **111** 3447
[21] Hu T, Zhang Q M, Wells J C, Gong X G and Zhang Z Y 2010 *Phys. Lett. A* **374** 4563
[22] Yuan J M, Hao W P, Li S H and Mao Y L 2012 *Acta Phys. Sin.* **61** 087301 (in Chinese)
[23] van Helden P and Ciobica I M 2011 *ChemPhysChem* **12** 2925
[24] Jang D E and Carter E A 2005 *Phys. Rev. B* **71** 045402
[25] Cinquini F, Delbecq F and Sautet P 2009 *Phys. Chem. Chem. Phys.* **11** 11546
[26] Liu X W, Huo C F, Li Y W, Wang J G and Jiao H J 2012 *Surf. Sci.* **606** 733
[27] Clark S J, Segall M D, Pickard C J, Hasnip P J, Probert M I J, Refson K and Payne M C 2005 *Z. Kristallogr.* **220** 567
[28] Segall M D, Lindan P J D, Probert M J, Pickard C J, Hasnip P J, Clark S J and Payne M C 2002 *J. Phys.: Condens. Matter* **14** 2717
[29] Perdew J P, Burke K and Ernzerhof M 1996 *Phys. Rev. Lett.* **77** 3865
[30] Monkhorst H J and Pack J D 1976 *Phys. Rev. B* **13** 5188
[31] Halgren T A and Lipscomb W N 1977 *Chem. Phys. Lett.* **49** 225